

NUMERICAL INVESTIGATION OF SURFACE WAVE TOMOGRAPHY
SCHEME FOR THREE-DIMENSIONAL INHOMOGENEITIES
RECONSTRUCTION

© 2025 D. D. Pozdnyakova^{a,*}, D. A. Presnov^b, A. S. Shurup^{a,b,c}

^a*Lomonosov Moscow State University, Moscow, Russia*

^b*Schmidt Institute of Physics of the Earth of the Russian Academy of Sciences, Moscow,
Russia*

^c*Shirshov Institute of Oceanology of the Russian Academy of Sciences, Moscow, Russia*

*e-mail: d_pozdnyakova@live.ru

Received September 06, 2024

Revised September 16, 2024

Accepted September 30, 2024

Abstract. A three-dimensional tomographic scheme for reconstructing parameters of inhomogeneous geophysical media is proposed. Initial data are propagation times of surface waves in various frequency ranges. Results of numerical modeling implemented for conditions of the Hawaiian Archipelago are presented, which indicate the operability of the proposed approach.

Keywords: *seismoacoustic tomography, surface wave, layered geophysical medium*

DOI: 10.31857/S03676765250125e8

INTRODUCTION

The study of volcanoes is an urgent and demanded task. Of particular interest is the monitoring of volcanic activity in densely populated areas. In some cases, such as at Merapi Volcano in Indonesia in 2010 [1], it was possible to obtain accurate estimates of the onset and intensity of eruptions, which allowed timely and prompt evacuation of the local population and saved thousands of human lives. The Kamchatka Branch of Geophysical Research of the Russian Academy of Sciences also has successful examples of realizing short-term forecasts of volcanic eruptions [2]. Seismoacoustic tomography is a key method of studying deep structures of the Earth, which allows to identify the structure and physical properties of rocks, as well as to observe changes in seismic parameters using a relatively small amount of data on the travel times of waves along different paths crossing the study area [3]. The use of surface seismic waves as a source of information about the geophysical environment led to the emergence of surface-wave tomography, which is currently used not only on land but also in ocean floor studies [4]. The fact that surface seismic waves attenuate slower with distance than bulk waves allows to use them for monitoring regions on both global and regional scales. Another peculiarity of surface waves is the dependence of their penetration depth on frequency, which makes it possible to obtain information on the characteristics of the medium located at different depths using a broadband sounding mode. Practical realization of such sounding is feasible by methods of noise interferometry [5, 6], which does not require the use of expensive low-frequency radiators. Usually, the surface-wave tomographic scheme consists of two stages: at the first stage, dispersion dependences of group or phase

velocities of surface waves are reconstructed at the points of the investigated region; at the second stage, the obtained dispersions are inverted into three-dimensional distributions of medium parameters. In the present work, we consider a one-stage three-dimensional tomographic scheme that skips the intermediate stage of dispersion dependence reconstruction. This approach allows to reduce the time of solution of the inverse three-dimensional problem, to reduce the requirements to the technical capabilities of the used computational systems; it also becomes possible to take into account the smoothness of the medium characteristics not only at different depths, but also in different geographical points. Modeling is carried out for the conditions of the PLUME experiment [7] with geophysical environment parameters corresponding to the Hawaiian archipelago [4]. The reconstruction of the three-dimensional shear wave velocity field by surface wave propagation times in different frequency ranges is considered.

PROBLEM STATEMENT

It is assumed that the sources and receivers exciting and registering surface waves are located in the region under consideration, the propagation trajectories of which cover the region under study quite densely (Fig. 1a). At the current stage of research, it is assumed that the influence of the water layer and bottom topography can be neglected in the frequency range under consideration; Rayleigh waves propagating along the boundary of a flat-layered medium are considered (Fig. 1b). The perturbation of the propagation times of the considered surface waves $\Delta t_i(f)$ is considered to be the difference between

the known experimental t_i^{exp} and calculated theoretical t_i^{teor} propagation times between i - source-receiver pairs at a given frequency f . The theoretical values t_i^{teor} are calculated for an a priori known "unperturbed" transverse wave velocity distribution, $c_s(\vec{r}) \vec{r} = \{x, y, z\}$ - a three-dimensional radius-vector. It is required to recover the deviation of the velocity $\Delta c_s(\vec{r})$ from its background value $c_s(\vec{r})$. The presence of $\Delta c_s(\vec{r})$ gives rise to $\Delta t_i(f)$. It is assumed that in the real situation $\Delta c_s(\vec{r})$ is small compared to $c_s(\vec{r})$, which allows us to say that there is a close to linear relationship between $\Delta c_s(\vec{r})$ and $\Delta t_i(f)$ [8]:

$$\Delta t_i(f) = t_i^{exp} - t_i^{teor} \sim \Delta c_s(\vec{r}). \quad (1)$$

To solve the reconstruction problem $\Delta c_s(\vec{r})$ from data $\Delta t_i(f)$, the inhomogeneities $\Delta c_s(\vec{r})$ are decomposed into basis functions: $\theta_j(\vec{r})$

$$\Delta c_s(\vec{r}) = \sum_{j=1}^J x_j \theta_j(\vec{r}), \quad (2)$$

where x_j are the unknown coefficients of the basis expansion. As a rule, the basis used in solving tomographic problems should satisfy the following requirements [9]: it can be used to describe the expected perturbations of the medium characteristics with the required accuracy and its use should not impose additional complexities or restrictions on the calculations performed. In the present work, a striped basis previously developed and used for hydroacoustic applications [9] is used. This basis was modified to solve the problem under consideration (Fig. 1b) in order to take into account the peculiarity of the tomographic scheme under consideration - the penetration of surface waves to different

depths at different frequencies allows for "layer-by-layer" sounding of the tomographic medium. The parameters of the Pacific Ocean lithosphere model (thicknesses of layers, densities, velocities of bulk waves in them) obtained in [4] are used. When constructing the baseline, each layer is divided into three-dimensional strips, also rotated with an equal angular step (Fig. 1b). The ratio of the number of strips P and rotation angles U is chosen from the requirement of mutual intersection of the peripheral parts of the baseline strips at one rotation or, to put it differently, the absence of areas between angle-adjacent strips that do not fall into any of them:

$$\frac{U}{P} \geq \frac{\pi}{2}. \quad (3)$$

The basis functions $\theta_j(\vec{r})$ represent "basis" perturbations of the transverse wave velocities localized in the basis strips.

A system of linear equations is considered to find the unknown coefficients of x_j (2):

$$AX = \Delta T, \quad (4)$$

where the experimentally measured perturbation times Δt_i form the column ; ΔT is the perturbation matrix whose elements are the calculated perturbations of the times Δt_{ij} of surface wave propagation between i a source-receiver pair in a medium with inhomogeneity given by the j basis function ; $\theta_j(\vec{r})$ X is the column of the coefficients of the expansion x_j of the three-dimensional inhomogeneity $\Delta c_s(\vec{r})$ by the basis functions $\theta_j(\vec{r})$. System (4) implies that the time perturbations Δt_i , found from the experiment and

caused by the presence of the desired inhomogeneity $\Delta c_s(\vec{r})$, can be represented as a linear combination of the time perturbations Δt_{ij} , also caused by the basis functions $\theta_j(\vec{r})$:

$$\Delta t_i = \sum_{j=1}^J \Delta t_{ij} x_j. \quad (5)$$

The regularized MNC solution of the system (4), (5) has the form:

$$\hat{X} = (A^+ A + \varepsilon E)^{-1} A^+ \Delta T, \quad (6)$$

where E is the unit matrix; ε is the Tikhonov regularization coefficient; the symbol "+" at the perturbation matrix A means Hermite conjugation. When solving the system (4), it is important that the number of unknowns $P \cdot U$, taking into account their coupling (3) does not exceed the total number of input data, which is determined by the number of source-receiver pairs and the number of frequencies used. This requirement can be relaxed by using additional independent information about the type of inhomogeneities to be reconstructed, such as inhomogeneity smoothness conditions $\Delta \hat{c}_s(\vec{r})$, implying that the values of the reconstructed functions should not vary in neighboring spatial points by any significant amount. The solutions found from (6) \hat{x}_j give an estimate of the sought inhomogeneities:

$$\Delta \hat{c}_s(\vec{r}) = \sum_{j=1}^J \hat{x}_j \theta_j(\vec{r}). \quad (7)$$

When solving the tomographic problem under discussion, the following assumptions were additionally taken into account. First, since the localization of surface waves depends on frequency, it is expected that at higher frequencies the wave will no

longer penetrate deeper layers. Thus, in the model under consideration (Fig. 2), layers located at depths noticeably greater than the wavelength should be excluded for the selected frequency range. Secondly, the reconstruction at a given frequency should use the basis bands at those depths for which the perturbation of the transverse wave velocity leads to appreciable change in the propagation time of the surface wave. In other words, the surface wave at the considered frequency should be "sensitive" to the perturbation of the reconstructed medium parameters at the considered depth. To verify these assumptions, numerical modeling was carried out. A medium consisting of plane-parallel layers was considered. On the boundary of the considered layered medium at a distance R from each other were located the source and the receiver. For the selected frequency f in each layer, a velocity perturbation was introduced in turn $\Delta c(z)$, after which perturbations of surface wave propagation times were calculated: Δt

$$\Delta t(f) = R \left(\frac{1}{c_0(z) + \Delta c(z)} - \frac{1}{c_0(z)} \right), \quad (8)$$

where $c_0(z)$ are the unperturbed values of the transverse wave velocity in the layers. Examples of modeling results (8) are presented in Fig. 2. According to the experiment processing data obtained in [4], a total of 17 frequencies in the range from 0.03 to 0.07 Hz were considered. The check at the highest frequency of 0.07 Hz showed that the use of the basis functions $\theta_j(\vec{r})$, located on layers lying below 12 km is not reasonable, since for them the time perturbation Δt increases with the growth of the velocity perturbation $\Delta c_s(\vec{r})$, which contradicts the linear approximation. Meanwhile, at a frequency of 0.03

Hz, it makes sense to consider all layers up to a depth of 80 km, corresponding to the deepest layer. As for the sensitivity assessment, at 0.03 Hz all considered layers are insensitive to variations of surface wave velocities, whereas at 0.07 Hz the only layer not rejected earlier, lying at a depth of 12 km, has a high sensitivity to these variations. A similar analysis was carried out for all considered frequencies, which allowed us to proceed to the solution of the inverse problem at the next step. Before that, it was of interest to study the resolving power not only in depth but also in the horizontal plane.

NUMERICAL MODELING OF TOMOGRAPHIC RECOVERY

The horizontal resolving power of the discussed surface-wave tomography scheme was checked using the "checkerboard" test [10]. The model is represented by alternating positive and negative disturbances in the form of adjacent squares with side 200 km and amplitude of 10% of the unperturbed transverse wave velocity in each layer; there is no alternation in depth (Fig. 3). The radius of the investigated area $R \approx 800$ km. The test was performed for two modifications of the striped baseline, each consisting of 12 layers, with the first modification of the baseline being $P = 8$ strips and $U = 15$ rotation angles on each layer, and the second modification being $P = 16$ $U = 27$. Fig. 3 shows the results of the synthetic checkerboard test on the example of a layer located at a depth of 40 km. From Fig. 3b, c shows that the resolution of the scheme increases with increasing number of basis elements. However, the increase in the number of basis elements is limited by the available amount of source data - the number of source-receiver pairs and the number of frequency bands used.

Further for modeling we used a modification of the striped basis with $P=16$ $U=27$. We considered 328 pairs of transducers arranged in the same way as in the PLUME experiment [7]. The initial surface wave propagation times were taken at 17 frequencies in the range from 0.03 to 0.07 Hz. It should be noted that controlled radiation at such low frequencies is hardly realizable in practice, and the chosen frequency range corresponds to passive correlation processing of natural seismoacoustic noise recorded in the PLUME experiment [4]. Fig. 4 shows the result of the reconstruction of two inhomogeneities with velocity perturbations opposite in sign:

$$c_s(x, y, z) = c_0(z) \left\{ 1 + \sum_{i=1}^2 \Lambda^{(i)} \exp\left(-\frac{(x - x_0^{(i)})^2 + (y - y_0^{(i)})^2}{2\sigma_{xy}^2}\right) \exp\left(-\frac{(z - z_0)^2}{2\sigma_z^2}\right) \right\}, \quad (9)$$

where $x_0^{(i)}$, $y_0^{(i)}$, $i = 1, 2$, z_0 , are the coordinates of the centers of inhomogeneities; σ_{xy} and σ_z are the RMS deviations in the horizontal and vertical planes, respectively; $\Lambda^{(i)}$, $i = 1, 2$ is the coefficient specifying the maximum deviation of velocity relative to the unperturbed value. For the case presented in Fig. 3a, $x_0^{(1)} = y_0^{(2)} = -200$ km, $x_0^{(2)} = y_0^{(1)} = 200$ km, $\sigma_{xy} = 200$ km, $\sigma_z = 15$ km, $\Lambda^{(1)} = -0.1$, $\Lambda^{(2)} = 0.1$. The solution of the direct problem is based on the application of the Thomson-Haskell matrix method of calculating dispersion curves over a given layered medium and the subsequent solution of the Eikonal equation for two-dimensional velocity maps at different frequencies [8]. A wave solution of the direct problem in the horizontal plane is also possible [11], which will improve the resolution but will require significantly more computational resources. The background medium was taken from [4], where the vertical profile of the transverse

wave velocity, average for the region under consideration, was obtained. The reconstruction involved zeroing the blocks of the perturbation matrix A , referring to the layers located at depths that do not contribute to $\Delta t_i(f)$, as well as taking into account the coupling equations between neighboring strips, rotation angles, and layers given by the following equation:

$$\frac{x_k - 2x_{k-1} + x_{k-2}}{2h} = 0, \quad (10)$$

where x_k, x_{k-1}, x_{k-2} are the expansion coefficients on "neighboring" basis bands located on nearby layers in depth, or located next to each other in one layer; h is the "smoothness" coefficient, which was set separately to control the smoothness of the reconstructed functions in depth and within the boundaries of one layer. Ratio (10) corresponds to the requirement of minimizing the second derivative of the reconstructed functions by spatial coordinates.

To assess the accuracy of the numerical simulation results obtained, the discrepancies were calculated by solving $\eta_{\Delta c}$:

$$\eta_{\Delta c} = \sqrt{\frac{\sum_{d,l,m} \left| \Delta c^{model}(x_d, y_l, z_m) - \Delta c^{rec}(x_d, y_l, z_m) \right|^2}{\sum_{d,l,m} \left| \Delta c^{model}(x_d, y_l, z_m) \right|^2}} \quad (11)$$

where Δc^{model} and Δc^{rec} are the given and reconstructed perturbations of the transverse wave velocity in the medium at discretized spatial points with coordinates x_d, y_l, z_m .

Fig. 4 presents the results of the reconstruction of the considered inhomogeneity (9). From Fig. 4b shows that the shape of inhomogeneities, their location, and amplitude values are reconstructed with acceptable accuracy. For the presented reconstruction variant, the discrepancy by the solution is $\eta_{\Delta c} = 0.27$, whereas without the coupling equations and zeroing the blocks of the perturbation matrix A the discrepancy value was $\eta_{\Delta c} = 0.51$, which indicates a noticeable improvement of the reconstruction results due to taking into account the peculiarities of the tomographic scheme discussed in the paper.

CONCLUSION

Thus, the results of numerical modeling presented in this paper indicate the possibility of restoring three-dimensional inhomogeneities using the developed surface-wave tomography scheme. In the presented work, the recovery of transverse wave velocities was considered, but the discussed approach can be developed for recovery of other medium characteristics for which a relation similar to (1) is valid. Of separate interest is the study of the possibilities of joint recovery of different medium parameters in the discussed approach. In the course of the "chess" test, the resolving power of two modifications of the striped basis was demonstrated, depending on the number of used basis elements, the number of which, in turn, is limited by the volume of the initial data. The advantages of optimizing the tomographic scheme by coupling equations and selecting only those layers that give the main contribution to the observed perturbations of surface wave propagation times are demonstrated. It is assumed that in the next stage

of the ongoing research the approach presented in this paper will be used for reconstruction from experimental data obtained during the PLUME experiment.

FUNDING

The research was supported by the grant of the Russian Science Foundation № 23-27-00271.

REFERENCES

1. *Jousset P., Pallister J., Boichu M. et al.* // *J. Volcanol. Volcanol. Geotherm. Res.* 2012. V. 241. P. 121.
2. *Koulakov I.Yu.* // *Russ. Geol. Geophys.* 2022. V. 63. No. 11. P. 1207.
3. *Yanovskaya T.B.* Surface-wave tomography in seismological research. SPb.: Nauka, 2015.
4. *Tikhotskii S.A., Presnov D.A., Sobisevich A.L., Shurup A.S.* // *Acoust. Phys.* 2021. V. 67. No. 1. P. 91.
5. *Dmitriev K.V.* // *Bull. Russ. Acad. Sci. Phys.* 2022. V. 86. No. 11. P. 1336.
6. *Dmitriev K.V.* // *Bull. Russ. Acad. Sci. Phys.* 2022. V. 86. No. 1. P. 94.
7. *Laske G., Markee A., Orcutt J.A. et al.* // *Geophys. J. Int.* 2011. V. 187. P. 1725.
8. *Presnov D.A., Sobisevich A.L., Shurup A.S.* // *Phys. Wave Phenom.* 2016. V. 24. No. 3. P. 249.
9. *Burov V.A., Sergeev S.N., Shurup A.S.* // *Acoust. Phys.* 2011. V. 57. No. 3. P. 344.
10. *Koulakov I.Yu., D'Auria L., Prudencio J. et al.* // *J. Geophys. Geophys. Res. Solid Earth.* 2023. V. 128. No. 3. Art. No. e2022JB025798.
11. *Zotov D.I., Rumyantseva O.D., Cherniaev A.S.* // *Bull. Russ. Acad. Sci. Phys.* 2024. V. 88. No. 1. P. 113.

FIGURE CAPTIONS

Fig. 1. Surface wave propagation trajectories between bottom seismic stations of the PLUME experiment used in the tomographic study (a) and modified strip-baseline (b).

Fig. 2. Numerical study of the linear relationship between the surface wave propagation time perturbation Δt and the transverse wave velocity perturbation Δc_s at frequencies of 0.03 Hz (a) and 0.07 Hz (b) at a fixed source-receiver distance.

Fig. 3. Synthetic "checkerboard test" model with maximum transverse wave velocity perturbation equal to 10% of the value in the undisturbed medium (a); recovery result using a striped basis modification containing 8 stripes and 15 rotation angles in a layer (b); same as (b), but the striped basis contains 16 stripes and 27 rotation angles in one layer (c).

Fig. 4. Initial distribution of inhomogeneities with the maximum perturbation of the transverse wave velocity equal to 10% of the value in the unperturbed medium (a); the result of reconstruction taking into account the coupling equations and excluding the blocks of the perturbation matrix with layers and frequencies for which the approximations used in the solution of the inverse problem are not fulfilled (b).

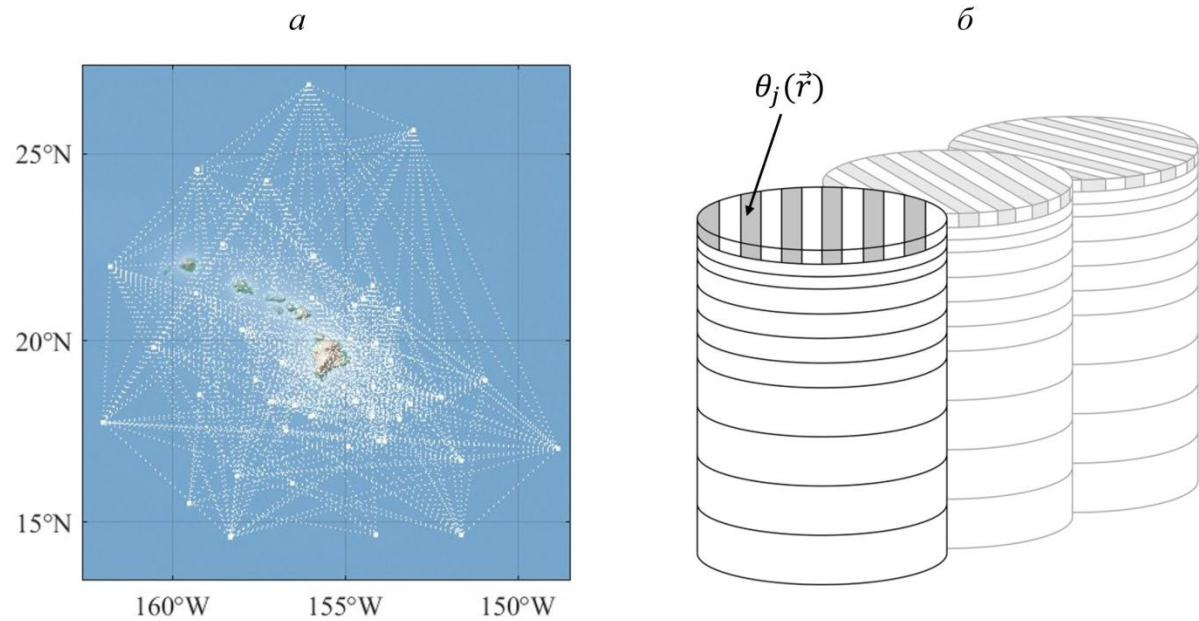


Fig. 1

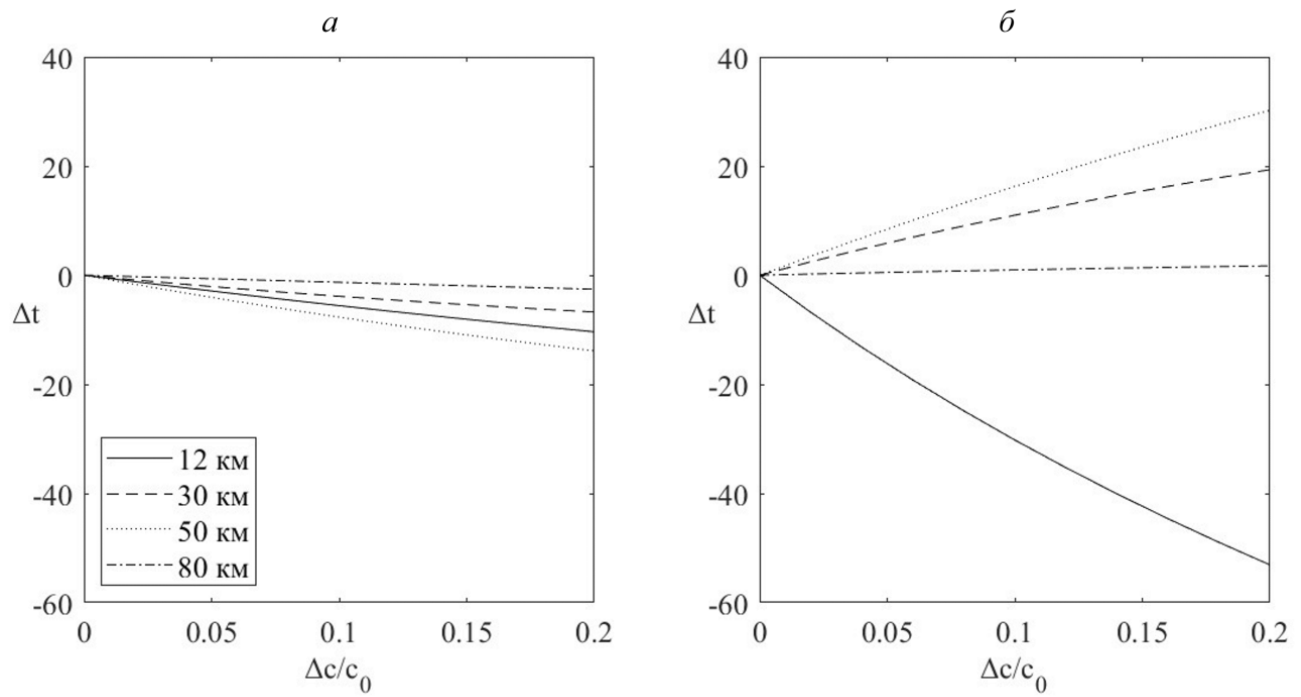


Fig. 2

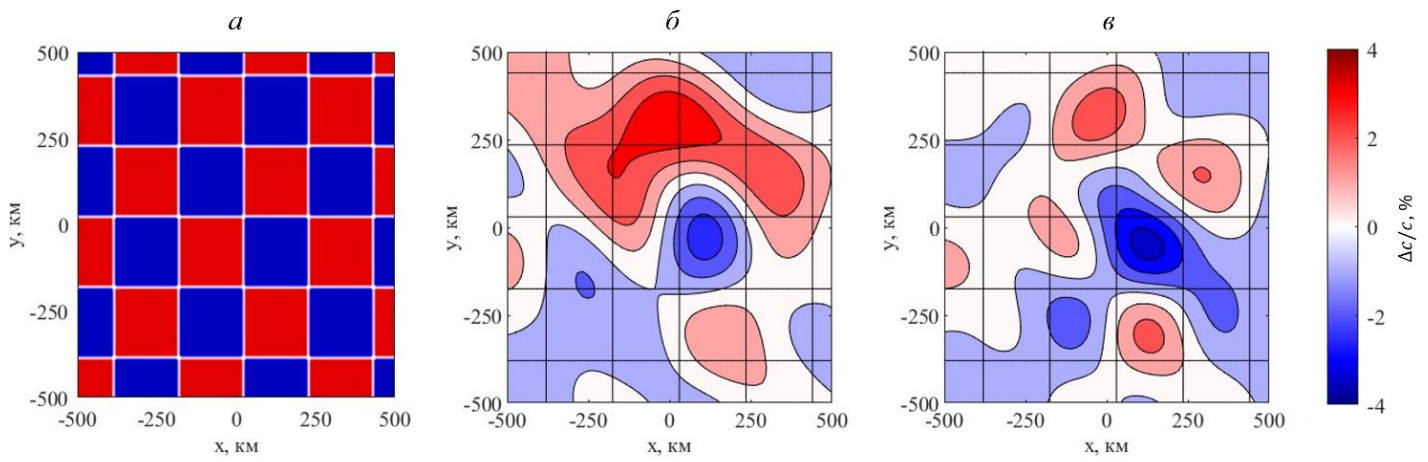


Fig. 3

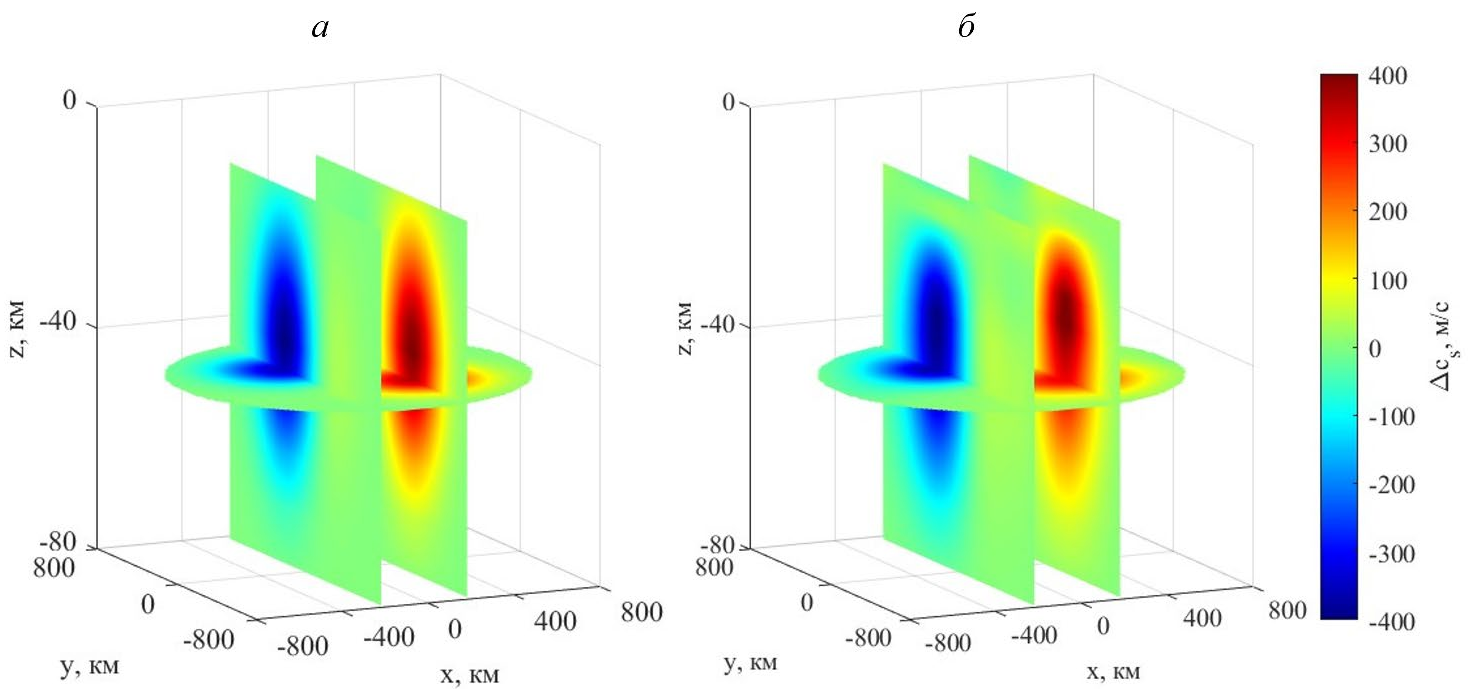


Fig. 4